Journal of Metals, Materials and Minerals, Vol. 32, No. 4, pp. 150-160, 2022

Sugarcane waste-derived activated carbon for lithium-sulfur batteries with enhanced performance by thiourea doping

Yanisa THUMKAEW,[1] Vipada PETSON,[1] Thanapat JORN-AM,[1] Natee SIRISIT,[1] Chalathorn CHANTHAD,[2] Jedsada MANYAM,[2] Xiao LIANG,[3] Shufeng SONG,[4] and Peerasak PAOPRASERT [1*]

[1] *Department of Chemistry, Faculty of Science and Technology, Thammasat University, Pathumthani, 12120 Thailand*
[2] *National Nanotechnology Center, National Science and Technology Development Agency, Pathumthani, 12120 Thailand*
[3] *State Key Laboratory of Chem/Bio-Sensing and Chemometrics, College of Chemistry and Chemical Engineering, Hunan University, Changsha, 410012 P.R. China*
[4] *School of Aerospace Engineering, Chongqing University, Chongqing, 400044 P.R. China*

***Corresponding author e-mail:** peerasak@tu.ac.th

Received date:
4 October 2022
Revised date
23 November 2022
Accepted date:
28 November 2022

Keywords:
Li-S battery;
Sugarcane;
Activated carbon;
Bagasse

Abstract

In this work, bio-renewable sugarcane bagasse and leaf were utilized for the preparation of activated carbon (BAC and LAC), which was then employed as the host material in lithium-sulfur (Li-S) batteries. The activated carbon, for the first time, was doped with nitrogen and sulfur via the addition of thiourea during the synthesis of carbon char via a simple, one-step hydrothermal method. The activated carbon was used to fabricate the cathodes of the CR2032 coin cells. The amount of added thiourea was found to influence the nitrogen/sulfur content, porosity, amorphous/graphitic structure, and performance of the activated carbon. At 0.2C, BAC2 (4.15 wt% thiourea doping) gave the highest specific capacity of 478 mAh·g^{-1} among the bagasse-derived activated carbon, while LAC3 (8.3 wt% thiourea doping) yielded the highest specific capacity of 521 mAh·g^{-1} among the leaf-derived activated carbon. They also demonstrated an excellent capacity retention of 72% and 83%, respectively, after 100 cycles. Furthermore, thiourea doping also improved the rate performance, by providing fast interfacial processes. Based on these results, the obtained activated carbon demonstrates the potential for the fabrication of high-performance Li-S batteries. Also, this work highlights the practical utilization of both sugarcane wastes for these emerging energy storage devices.

1. Introduction

Concerning energy security as well as the increasing use of fossil fuels, renewable energy sources are getting much attention. Energy production requires low cost, high-performance energy storage systems. For this reason, the development of such energy storage devices is needed. Despite low cost and high theoretical energy density, the development of Li-S batteries from renewable sources is important to drive further attention to these energy storage devices. Li-S batteries have become a focal point of research attention as they consist of lithium as an anode and naturally abundant sulfur as a cathode material, which is abundant and cheap. Sulfur has a theoretical energy density of 2600 Wh·kg^{-1} and a specific capacity of 1675 mAh·g^{-1} [1,2]. Mechanistically, the lithium anode dissolves during discharge, resulting in electrons and lithium ions being produced. Lithium ions are then transported to the cathode, causing the sulfur stored in the cathode to be reduced to lithium polysulfide and lithium plating back to the anode while charging [3]. Li-S batteries are notorious for poor cycling stability due to a phenomenon known as the shuttle effect. This is caused by the reduction of sulfur from S_8 to S_{n2} [4], which results in irreversible sulfur when the discharge voltage reaches 2.3 V [5]. As the voltage drops to 1.9 V, the lithium polysulfides, Li_2S_8, Li_2S_6, and Li_2S_4, are converted into insoluble Li_2S_2 and Li_2S, resulting in corrosion at the negative electrode [6].

Due to the limitations of Li-S batteries, materials, such as activated carbon, have been employed as the porous hosts of sulfur to overcome the short lifetime of this type of batteries. Activated carbon has a high specific surface area due to its small pore size [7,8]. It is therefore used in a wide variety of applications, such as chemical adsorption [9], wastewater treatment [10,11], gas storage [8,12,13], and energy storage [14,15]. In addition, it has the advantages of low toxicity, high thermal stability, high-corrosion resistance, and facile synthesis. Furthermore, its porosity can be tuned via the choice of raw materials or preparation methods/conditions. Activated carbon can be prepared via physical or chemical activation. Physical activation is a two-step process that involves carbonization in the atmosphere and uses gases, such as water vapor and carbon dioxide, to induce oxidizing gases in the atmosphere at high temperatures (800°C to 1100°C) [16]. Chemical activation uses chemical activating agents to create porosity and is widely used for biomass materials. Examples of chemical activating agents are KOH [17], NH_3 [18], and NaOH [19]. The pores are formed as the chemical activator can penetrate deeply into the

carbon structure under high-temperature inert gas (400°C to 900°C) [20]. The advantages of physical activation include being an inexpensive and toxic chemical-free method [21]. The disadvantages are the low adsorption capacity, long activation time, and high energy consumption [22,23]. Chemical activation has the disadvantage of using oxidizing chemicals, such as KOH and NaOH, which are more toxic, corrosive, and expensive than CO_2 and H_2O and require a final rinse for removal. Nonetheless, chemical activation is still widely used to make activated carbon for a range of applications.

Sugarcane is regarded as an important economic crop and an efficient sugar-producing source. Sugarcane is grown in tropical areas in several countries all over the world. Thailand is one of the major sugarcane cultivating countries. The area for sugarcane cultivation has increased in every region of the country because sugar is also the chemical precursor and building block for various compounds [24] . As sugarcane is used to produce sugar, there are by-products, such as bagasse and leaf, after harvesting and sugar production. Only a small quantity of bagasse finds some uses, such as fuel and food containers. Even worse, the leaf currently has very little use and is often burned for the next cultivation process, causing pollution and greenhouse gases [25]. Therefore, it is a challenge to maximize the use of sugarcane wastes and also to solve the problems of eliminating wastes that disrupt the world's environment. Bagasse and sugarcane leaf are considered ideal sources for the preparation of activated carbon. Bagasse and sugarcane leaf contain lignocellulose, which is considered to be an organic biomass. Lignocellulose-containing materials produce a solid residue (char) during carbonization, which is convenient for the synthesis of porous activated carbon [26]. Therefore, sugarcane wastes are suitable sources for activated carbon production.

In this work, we synthesized activated carbon from sugarcane bagasse and leaf and used it as a host material for sulfur in the cathode of Li-S batteries (Figure 1). Although bagasse has been used [27-30], the leaf has not been reported in Li-S batteries. Thiourea was used as a dopant to incorporate nitrogen and sulfur into the activated carbon, which, to the best of our knowledge, is reported for the first time for Li-S batteries. The effects of the thiourea amount on the battery performance were studied. Performance comparison between bagasse- and leaf-derived activated carbon was discussed. This work demonstrates a low-cost strategy for converting sugarcane wastes into Li-S batteries. The findings from this work will be useful for the development of high-performance energy storage devices from bio-renewable sources.

Figure 1. Schematic representation of this work.

2. Experimental

2.1 Materials

The sugarcane bagasse and leaf were acquired from the neighborhood farmer's market in Pathum Thani, Thailand. All chemical compounds were reagent grade and were utilized directly.

2.2 Synthesis of activated carbon

The method employed in the prior work to prepare the activated carbon from sugarcane bagasse and leaf as raw materials was followed [31]. 6 g of raw materials were chopped into small pieces. After being cleaned with distilled water, they were dried at 80°C for 12 h. Thiourea (0 wt% to 16.6 wt%) was dissolved in a 75 mL solution of sulfuric acid. The raw materials were then combined with the thiourea solution, sealed in an autoclave, and heated at 180°C for 8 h. The mixture was filtered to remove the solid component, and then rinsed with deionized water before drying at 80°C overnight in a vacuum oven. The solid product was impregnated with KOH at a mass ratio of 1:1 in a crucible and then heated inside a tube furnace at 800°C for 2 h under nitrogen atmosphere.

2.3 Preparation of electrode

The mixture between activated carbon and sulfur (1:1 ratio by weight) was prepared. With *N*-methyl-2-pyrrolidone as the solvent, 80% mixture, 10% carbon black, and 10% polyvinylpyrrolidone as a binder were combined to form a slurry. The slurry was coated on aluminum foil and used as a cathode after drying at 60°C for 12 h in an oven. The counter electrode consists of lithium metal foil. Celgard 2300 was used as the separator. Lithium bis(trifluoromethanesulfonyl) imide was dissolved in a mixture of 1,3-dioxolane and dimethyl ether and used as an electrolyte.

2.4 Characterization

The activated carbon was characterized using a Raman spectrometer (NT-MDT, NTEGRASpectra model). X-ray diffraction (XRD) analysis was performed using the RigakuD/max2550VL/PC system. The surface morphology was examined using a scanning electron microscope (SEM, Hitachi, S-3400) with a 15 kV accelerating voltage. Using a Quantachrome, Autosorb iQ-C analyzer, the surface areas and pore size distribution were determined using the N_2 adsorption/desorption isothermal method. The Brunauer-Emmett-Teller (BET) surface area was calculated using the Brunauer-Emmett-Teller (BET) model, while the pore volume and pore size distribution were produced using the Barret-Joner-Halenda (BJH) approach.

2.5 Electrochemical measurements

The battery cells were assembled in an argon-filled glove box. The cycling voltammetry of the cells was performed at a 0.01 mV scan rate. Galvanostatic charge-discharge cycles in the voltage range of 1.5 V to 2.8 V and electrochemical impedance studies were performed over a frequency range between 10^{-1} to 10^{5} Hz.

3. Results and discussion

3.1 Characterization of activated carbon

Sugarcane bagasse and leaf served as the starting materials for the hydrothermal process that produced activated carbon with sulfuric acid acting as a catalyst. Crystalline cellulose and hemicellulose were hydrolyzed and dissolved under the high pressure and temperature of the hydrothermal treatment. These materials were carbonized with the assistance of sulfuric acid to form the carbon char. With the addition of thiourea, the hydrothermal technique produced N,S-doped carbon char. After that, KOH was used as an activating agent to chemically activate the char. KOH etched off the carbon char, helped by a high temperature and an inert environment, to create extremely porous carbon structures [32-34]. The activated carbon was collected with 31% to 36% yields (Table 1).

SEM was used to analyze the morphology and structure of bagasse, leaf, carbon char, and activated carbon. The sugarcane bagasse and leaf are depicted in Figure 2(a-b). According to Figure 2(c-d), the carbon char made from bagasse and leaf looked to be rougher than the bagasse and leaf, confirming that following hydrothermal treatment, the bagasse and leaf experienced structural alteration. The carbon char that had been exposed to thiourea showed spherical formations with size between 20 nm and 30 nm (Figure 2(e-f)). The hydrothermal technique is what gives the carbon char its spherical form [35]. This demonstrates a quick approach for making carbon spheres without the need for complicated tools or laborious procedures. Under high temperature and pressure, the bagasse and leaf residues underwent nucleation, carbonization, and isokinetic development to produce carbon spheres, with these processes being favorably thermodynamically driven by negative Gibb's free energy [36]. The carbon sphere might collapse if the reaction time was prolonged. Since our carbon spheres clearly did not go through the collapse process, the hydrothermal treatment at 180°C for 8 h resulted in the formation of well-defined carbon spheres. The shape of the activated carbon after the activation process is shown in Figure 2(g-n). As a result of the destruction of the carbon spheres, irregular structures of activated carbon were left behind, and some of which still contained residues of the carbon spheres. This suggests that highly porous materials were formed following the activation.

Figure 3(a-b) depict the Raman spectra of the activated carbon. The existence of disordered and crystalline graphitic carbon was shown by the D and G bands, respectively. The D band is recognized as the peak at 1337 cm^{-1}, while the G band is located at 1620 cm^{-1}. Because the G band is present, it is possible to employ the activated carbon made from bagasse and leaf as electrodes in a supercapacitor because it is electrically conductive. The structural defects in heteroatoms connected to sp^3 carbon are determined by the D and G band ratio (I_D/I_G) [37] (Table 2). Thiourea successfully decreased the quantity of disordered or amorphous carbon while increasing the amount of graphitic carbon, as evidenced by the fact that increasing the amount of thiourea decreased I_D/I_G ratios. It is anticipated that the use of thiourea dopant might assist the formation of graphitic carbon and ordered structure, thereby lowering I_D/I_G ratios as a result.

Figure 3(c-d) show the XRD patterns of the activated carbon made from bagasse and leaf. The amorphous carbon structures are responsible for the distinctive peak between 15° to 30°, denoted as C(002). The C(101) diffraction peak due to the graphitic structure is indicated by the weak and broad band between 40° to 50° [38]. Table 3 displays the chemical compositions of carbon char and activated carbon. Due to the use of thiourea as a dopant, all samples contained nitrogen and sulfur. The carbon char had a high content of sulfur, but this quantity greatly diminished after the activation process. The amount of sulfur in activated carbon decreased as a result of the volatile sulfur compounds that were produced during the high-temperature activation [39]. The activated carbon samples made from bagasse and leaf, respectively, showed the highest nitrogen and sulfur concentrations in BAC2 and LAC4, respectively. The fact that the nitrogen and sulfur concentrations did not correspond with the amounts of added thiourea indicates that the majority of the volatiles comprising nitrogen and sulfur were produced and released during the high-temperature activation process. However, these outcomes show that the N,S-doped activated carbon made from sugarcane bagasse and leaf was successfully synthesized.

The characteristics of activated carbon's surface area, pore volume, and pore size were then determined. The type-IV BET isotherms show that the activated carbon is a mesoporous substance (Figure 4(a-b). It was discovered that the surface area of activated carbon made from bagasse increased with thiourea concentration, but that of activated carbon made from leaf dropped (Table 4). It is generally known that the bagasse contains less lignin than the leaf but more cellulose chemicals [40]. These findings show that the surface area and porosity of the produced activated carbon were significantly influenced by the various amounts of cellulosic components, lignin, and bagasse, as well as the amount of thiourea. According to this research, the amount of thiourea can be adjusted to modify the surface area and pore size, offering a different method for manufacturing activated carbon. High surface area and pore volume are necessary for sulfur storage [41].

Table 1. Reaction conditions for the preparation of activated carbon.

Raw material	Thiourea (%w/w)	Activated carbon	
		Code	Yield (%)
Bagasse	0	BAC1	31
Bagasse	4.15	BAC2	32
Bagasse	8.3	BAC3	32
Bagasse	16.6	BAC4	33
Leaf	0	LAC1	31
Leaf	4.15	LAC2	36
Leaf	8.3	LAC3	34
Leaf	16.6	LAC4	31

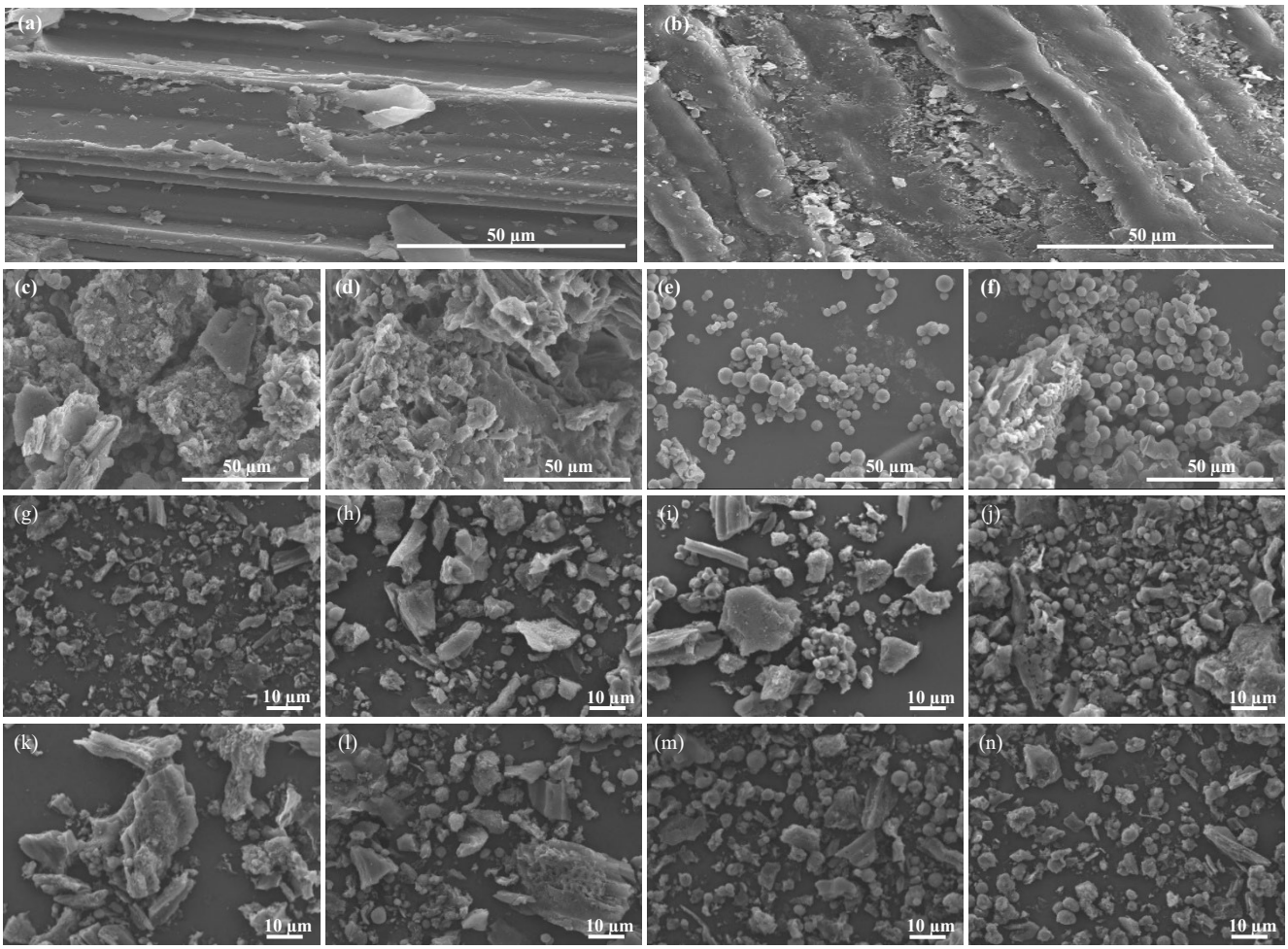

Figure 2. SEM images of (a) bagasse, (b) leaf (c) bagasse char of BAC1, (d) leave char of LAC1, (e) bagasse char of BAC2, (f) leave char of LAC3, (g) BAC1, (h) BAC2, (i) BAC3, (j) BAC4, (k) LAC1, (l) LAC2, (m) LAC3, and (n) LAC4.

Table 2. D bands, G bands, and I_D/I_G ratios of activated carbon.

Sample	D (cm^{-1})	G (cm^{-1})	I_D/I_G
BAC1	1320	1618	2.69
BAC2	1322	1615	1.57
BAC3	1317	1618	1.14
BAC4	1318	1619	1.14
LAC1	1317	1590	2.91
LAC2	1324	1606	1.78
LAC3	1320	1609	1.15
LAC4	1313	1616	1.17

Table 3. CHNS analysis of carbon char and activated carbon.

Sample	Elemental composition (%)			
	C	H	N	S
Char B-3	34.43	4.54	1.56	11.87
Char L-3	25.52	4.85	1.42	12.11
BAC1	82.53	1.42	0.76	1.72
BAC2	77.53	1.03	1.47	3.58
BAC3	86.59	0.63	0.90	0.91
BAC4	84.39	0.58	1.00	0.85
LAC1	80.54	1.14	0.80	1.67
LAC2	82.29	0.69	0.74	1.83
LAC3	80.11	0.59	1.00	0.67
LAC4	75.64	1.50	2.40	2.96

Table 4. Surface area and porosity of activated carbon made from bagasse and leaf.

Sample	Surface area ($m^2 \cdot g^{-1}$)	Pore volume ($cm^3 \cdot g^{-1}$)	Pore size (nm)
BAC1	602	0.486	15.285
BAC2	867	0.465	15.264
BAC3	1270	2.852	15.262
BAC4	1994	1.252	17.040
LAC1	2137	1.342	17.044
LAC2	1713	0.769	15.311
LAC3	1131	0.852	15.287
LAC4	803	0.357	28.163

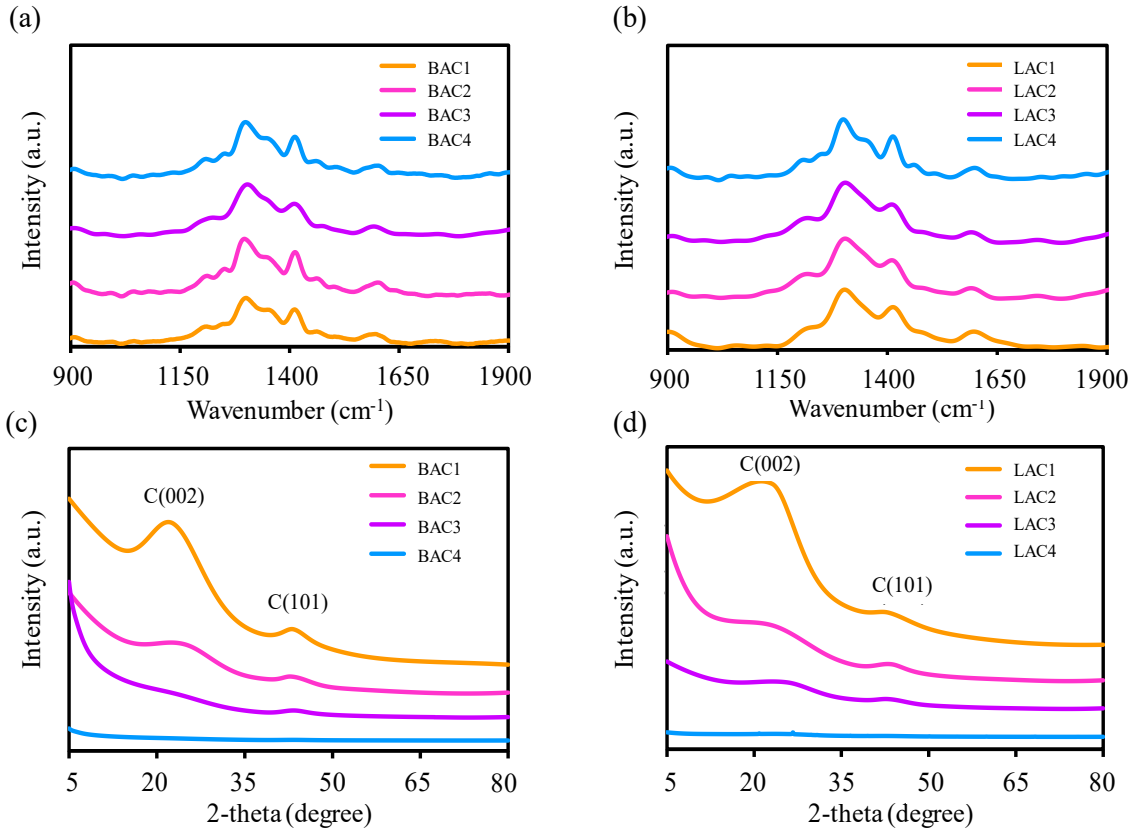

Figure 3. (a, b) Raman spectra and (c, d) XRD patterns of BACs and LACs.

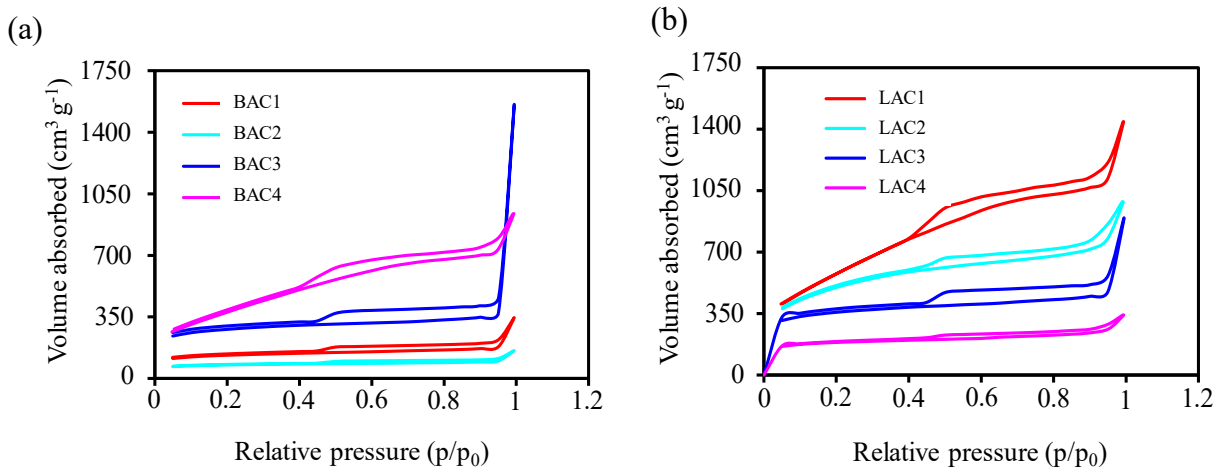

Figure 4. (a, b) N_2 adsorption–desorption isotherms of BACs and LACs.

3.2 Electrochemical performance

Activated carbon derived from sugarcane bagasse and leaf was used for the cathode preparation for Li-S batteries. The electrochemical performance of the BAC and LAC batteries was evaluated using cyclic voltammetry. As in Figure 5(a-b), they were recorded between 1.5 V and 3.0 V at a scan rate of 0.1 $mV{\cdot}s^{-1}$. The CV profiles demonstrated the sulfur cathode's normal electrochemical characteristics. Based on the oxidation peak from 2.30 V to 2.50 V, the BAC and LAC batteries revealed the conversion of lithium polysulfides to the metallic Li and S_8 [42,43], and the CV curves also revealed two reduction peaks at 2.3 V and 2.0 V derived from a stepwise reduction from S_8 to long-chain polysulfide Li_2S_x ($4<x<8$) and then to insoluble Li_2S [44]. Among the activated carbon made from bagasse and leaf, respectively, BAC2 and LAC3 displayed the largest CV responses, indicating the best redox and charge storage characteristics and well-pronounced electrochemical processes in the battery cells. These results also confirmed the typical functions of the fabricated batteries.

The cycling performance of BAC and LAC batteries is displayed in Figure 5(c-d). Apparently, the use of thiourea as the dopant in an appropriate amount resulted in higher capacity, compared to the activated carbon without thiourea doping, as shown in Figure 5(e-f). The initial capacities of the BAC1 and LAC1 batteries at 0.05C were 711 $mAh{\cdot}g^{-1}$ and 789 $mAh{\cdot}g^{-1}$ (Table 5). After 3 cycles, the current density was switched to 0.2C and the specific capacities dropped to 422 $mAh{\cdot}g^{-1}$and 412 $mAh{\cdot}g^{-1}$, respectively. This is typical because of a slow redox mechanism of charge storage in Li-S batteries. After 100 cycles, only 282 $mAh{\cdot}g^{-1}$ and 150 $mAh{\cdot}g^{-1}$ were retained, indicating that the capacity decay was fast. In contrast, the BAC2 and LAC3 batteries delivered the initial capacities of 856 $mAh{\cdot}g^{-1}$ and 939 $mAh{\cdot}g^{-1}$ at 0.05C and 617 $mAh{\cdot}g^{-1}$ and 630 $mAh{\cdot}g^{-1}$ at 0.2C, respectively. After 100 cycles, the BAC2 and LAC3 batteries gave a specific capacity of 478 $mAh{\cdot}g^{-1}$ and 521 $mAh{\cdot}g^{-1}$ at 0.2C, which are much better than the undoped activated carbon. The BAC2 and LAC3 capacity retentions are equivalent to 72% and 83%, respectively, which are better than BAC1 and LAC1 (67% and 36%, respectively). Polar interactions between N,S-doped activated carbon and elemental sulfur also provided an enhanced cycling stability [45]. The activated carbon containing nitrogen and sulfur within the framework demonstrated the ability to retain sulfur during charge/discharge cycles and accelerated the charge transfer processes for the excellent surface reactions required for charge transport and storage in cathodes [46]. These results demonstrate the potential of thiourea-doped activated carbon for Li-S batteries. Because LAC3, which gave the best performance, did not contain the highest amounts of nitrogen and sulfur, the doping concentration is not the only key factor here. In addition to nitrogen/sulfur content, we believe that the amount of added thiourea affected the surface area and porosity of the activated carbon, which in turn affected the battery performance. BAC1 and BAC4 gave poor performances among the bagasse-derived activated carbon, possibly because BAC1 had too small surface area while BAC4 had too large surface area. BAC3 yielded the best performance possibly due to the largest pore volume that could accommodate reactions of lithium polysulfides. Similarly, LAC2 produced the worst performance among the leaf-derived activated carbon because of its large surface area and small pore volume, while LAC3 had a sufficiently large pore volume to accommodate lithium polysulfides, resulting in the highest capacity. Therefore, pore volume is an important factor, controlling the battery performance. In addition, it is noteworthy to point out the graphitic carbon content of the activated carbon, characterized by Raman spectroscopy, also played a key role. LAC3 possessed the highest graphitic carbon among the leaf-derived activated carbon gave the best battery performance. Similarly, BAC2, which has a large amount of graphitic carbon, also gave the best battery results. These results suggested the graphitic carbon also influenced the battery performance by improving electrical conductivity. We can briefly conclude that the suitable amount of thiourea produced the activated carbon with appropriate nitrogen/sulfur concentration, surface area, porosity, and graphitic carbon that are suitable for hosting the sulfur in the framework and transferring charges. These contributing factors must be tuned by optimizing the amount of thiourea dopant in order to achieve the best battery performance. It is also important to point out that all fabricated batteries have an excellent coulombic efficiency over 99%, indicating an efficient and reversible charge/discharge cycle.

Electrochemical impedance characteristics of bagasse- and leaf-derived AC batteries were measured as shown in Figure 5(g-h). The BAC and LAC cells showed semicircles in the Nyquist diagram, representing the charge transfer resistance [47,48], respectively. The charge transfer resistance for the bagasse-derived AC electrodes can be ranked as follows: BAC2 < BAC4 < BAC3 < BAC1 and the leaf-derived AC electrodes can be ranked as follows: LAC3 < LAC2 < LAC4 < LAC1. It is obvious that the undoped activated carbon has the larger semicircles than the N,S-doped activated carbon, indicating that nitrogen/sulfur doping reduced the charge transfer resistance. The charge transfer resistance agreed well with the battery performance, in which BAC2 and LAC3 have the lowest resistance, giving rise to the highest battery performance. Despite having the highest charge transfer resistance, BAC1 and LAC1 were not the poorest in terms of the specific capacity, indicating that other factors also played an important role in governing the battery performance. Again, this confirms that the appropriate concentration of nitrogen/sulfur, surface area, porosity, and graphitic carbon contributed to the enhanced performance of the activated carbon.

Because BAC2 and LAC3 are the best among the bagasse- and leaf-derived activated carbon, they were further investigated and compared with BAC1 and LAC1, respectively. The discharge profiles of the fabricated batteries were measured, which can be separated into three regions, including the upper plateau at 0 $mAh{\cdot}g^{-1}$ to 180 $mAh{\cdot}g^{-1}$ (~2.3 V), the second plateau at 181 $mAh{\cdot}g^{-1}$ to 266 $mAh{\cdot}g^{-1}$ (~2.1 V), and the sloping region at 267 $mAh{\cdot}g^{-1}$ to 900 $mAh{\cdot}g^{-1}$ (< 2.0 V) (Figure 6(a-d)) [42,43]. The first two regions belonged to Li_2S_6 and Li_2S_4, respectively, while the third belonged to Li_2S. BAC2 and LAC3 had the higher discharge capacities than BAC1 and LAC1, especially on the upper and second plateaus. These results indicate that the N,S-doped activated carbon enhanced the charge storage capacity through favorable lithium polysulfide formation. This confirms that our thiourea-doped activated carbon prepared from sugarcane wastes acted as a good host material for Li-S batteries and outperformed the undoped activated carbon.

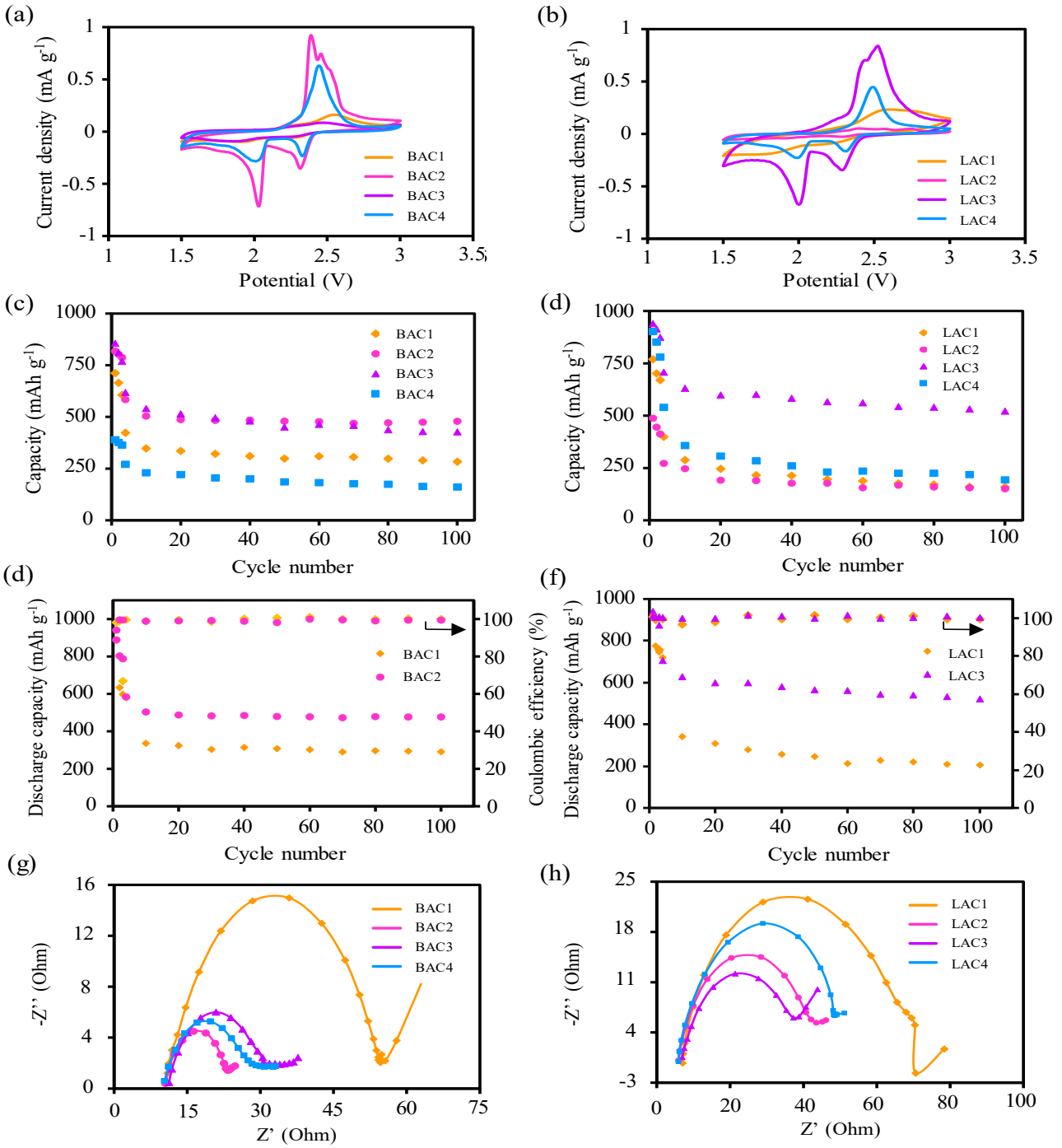

Figure 5. (a, b) CV curves of BAC and LAC batteries at a scan rate of 0.01 $mV{\cdot}s^{-1}$, (c, d) cycling stability of BAC and LAC batteries (1^{st}-3^{rd} cycles at 0.05C and 4^{th}-100^{th} cycles at 0.2C), (e, f) the cycling performance and coulombic efficiency (1^{st}-3^{rd} cycles at 0.05C and 4^{th}-100^{th} cycles at 0.2C), and (g, h) Nyquist plots.

Table 5. Specific capacities of BAC and LAC batteries.

Sample	Capacity at 1^{st} cycle at 0.05C ($mAh{\cdot}g^{-1}$)	Capacity at 1^{st} cycle at 0.2C ($mAh{\cdot}g^{-1}$)	Capacity at 100^{th} cycle at 0.2C ($mAh{\cdot}g^{-1}$)
BAC1	711	422	282
BAC2	812	540	478
BAC3	856	617	407
BAC4	364	230	161
LAC1	789	412	150
LAC2	487	271	151
LAC3	939	630	521
LAC4	851	539	162

The rate performances of BAC1, BAC2, LAC1, and LAC3 batteries are displayed in Figure 6(e-f). The BAC2 cathode delivered the much better capacities at all current densities, indicating better rate performance than BAC1. Also, LAC3 gave a better rate performance than LAC1. These results confirmed that nitrogen/sulfur doping of the activated carbon enhanced the Li-S battery performance. Comparing between BAC2 and LAC3, BAC2 showed a better rate performance than LAC3, especially at a high current density of 1C because the capacity of LAC3 dropped to nearly zero. Specifically, at 1C current density, the specific capacities of BAC2 and LAC3 are 233 mAh·g^{-1} and 3 mAh·g^{-1}. These results indicate that LAC3 possessed poorer interfacial kinetics that led to more sluggish redox reactions in response to the high applied current, as compared to BAC2 [49]. This also suggests that BAC2 is more suitable for applications that require fast charge and discharging. The value of BAC2 is impressive as it is comparable to that of a commercial lithium-ion battery. When the current density was switched back to 0.05C, the specific capacity recovered almost to the initial values, indicating a good charge storage recovery. Overall, we demonstrated that the bagasse- and leaf-derived activated carbon can be utilized in Li-S batteries and in terms of rate performance, and the activated carbon prepared from the bagasse showed better rate performance than that prepared from the leaf. Regarding to the economic feasibility, it is highly possible for our strategy and development to be applied for large scale and real applications by the following reasons: 1) the sugarcane bagasse and leaf are low cost materials and so is thiourea, 2) the hydrothermal method for the production of carbon char and KOH activation are applicable for large scale utilization because they are straightforward thermal-based methods, 3) the percent yields of the resulting activated carbon are high, and 4) the developed Li-S batteries are as good as the commercial lithium-ion batteries. For these reasons, we are confident that our batteries are economically feasible.

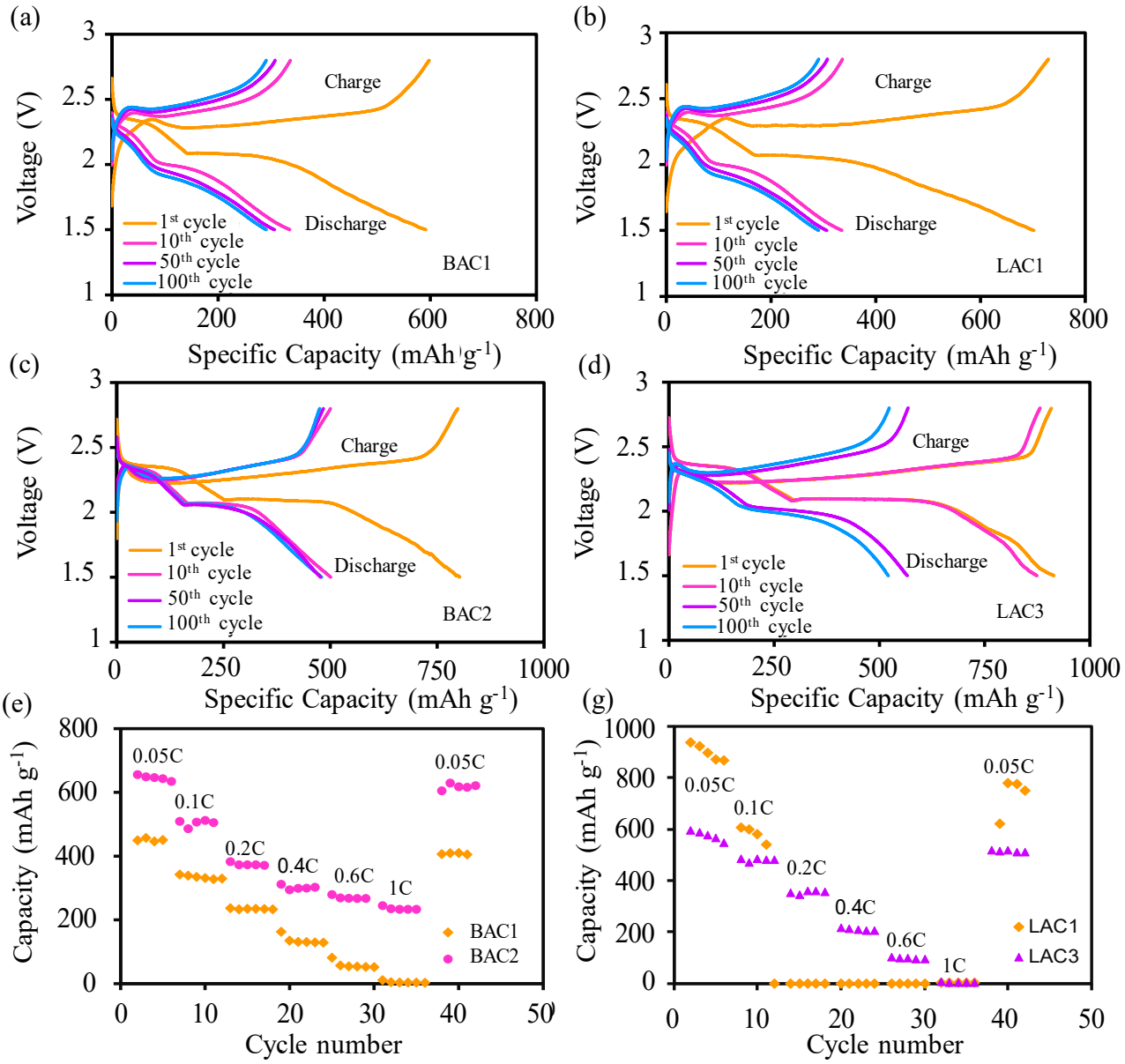

Figure 6. (a-d) Charge/discharge profiles under various cycles at 0.2C rate and rate performance (e, f) from 0.05C to 1C of BAC1, BAC3, LAC1, and LAC3 batteries, respectively.

4. Conclusions

Activated carbon derived from sugarcane bagasse and leaf, considered as abundant biomass materials, was prepared by the hydrothermal method and thermal activation. Thiourea was used as a dopant to incorporate nitrogen and sulfur into the activated carbon. The N,S-doped activated carbon was found to improve the specific capacity, cycling stability, and rate performance of the Li-S batteries. The leaf-derived activated carbon yielded a slightly better specific capacity but a lower rate performance than the bagasse-derived activated carbon. Both sources of activated carbon provided excellent capacity retention over 70% after 100 cycles. In addition, the amount of thiourea dopant also governed the performance of the batteries for both sources of activated carbon and the appropriate amount is needed to produce the best battery performance. Nonetheless, both sugarcane bagasse and leaf showed the potential to be used as raw materials for the preparation of activated carbon for Li-S batteries. Also, thiourea was demonstrated to be the potent dopant, enhancing the performance of this promising energy storage device. Future development includes surface engineering of activated carbon for improving the stability and lifetime of the Li-S batteries.

Acknowledgements

This study was supported by National Research Council of Thailand (contract No. W2E-04-63).

References

[1] R. Kumar, J. Liu, J.-Y. Hwang, and Y.-K. Sun, "Recent research trends in Li-S batteries," *Journal of Materials Chemistry A,* vol. 6, 2018.

[2] W. Ren, W. Ma, S. Zhang, and B. Tang, "Recent advances in shuttle effect inhibition for lithium sulfur batteries," *Energy Storage Materials,* vol. 23, pp. 707-732, 2019.

[3] Y. Zhao, H. Yin, Z. Zhang, C. Lyu, X. Zhao, H. Xu, G. Lu, T. Qin, G. Ouyang, C. Zha, and L. Wang, "Self-limiting lithiation of vanadium diboride nanosheets as ultra-stable mediators towards high-sulfur loading and long-cycle lithium sulfur batteries," *Sustainable Energy & Fuels,* vol. 5, no. 12, pp. 3134-3142, 2021.

[4] X. Tang, R. Gan, L. Tan, C. Tong, C. Li, and Z. Wei, "3D net-like GO-d-Ti_3C_2Tx mxene aerogels with catalysis/adsorption dual effects for high-performance lithium–sulfur batteries," *ACS Applied Materials & Interfaces,* 2021.

[5] P.-P. R. M. L. Harks, T. W. Verhallen, C. George, J. K. Van Den Biesen, Q. Liu, M. Wagemaker, and F. M. Mulder, "Spatiotemporal quantification of lithium both in electrode and in electrolyte with atomic precision via operando neutron absorption," *Journal of the American Chemical Society,* vol. 141, no. 36, pp. 14280-14287, 2019.

[6] D. Moy, A. Manivannan, and S. Narayan, "Direct measurement of polysulfide shuttle current: A window into understanding the performance of lithium-sulfur cells," *Journal of the Electrochemical Society,* vol. 162, pp. A1-A7, 2015.

[7] T. Mays, "A new classification of pore sizes," *Studies in Surface Science and Catalysis* vol. 160, pp. 57-62, 2007.

[8] M. Jung, J. Park, K. Lee, N. F. Attia, and H. Oh, "Effective synthesis route of renewable nanoporous carbon adsorbent for high energy gas storage and CO_2/N_2 selectivity," *Renewable Energy,* vol. 161, pp. 30-42, 2020.

[9] O. S. Nille, A. S. Patil, R. D. Waghmare, V. M. Naik, D. B. Gunjal, G. B. Kolekar, and A. H. Gore, "Chapter 11 - valorization of tea waste for multifaceted applications: A step toward green and sustainable development," in *Valorization of agri-food wastes and by-products*, R. Bhat Ed.: Academic Press, 2021, pp. 219-236.

[10] G. Jaria, V. Calisto, V. I. Esteves, and M. Otero, "Overview of relevant economic and environmental aspects of waste-based activated carbons aimed at adsorptive water treatments," *Journal of Cleaner Production,* vol. 344, p. 130984, 2022.

[11] J. Jjagwe, P. W. Olupot, E. Menya, and H. M. Kalibbala, "Synthesis and application of granular activated carbon from biomass waste materials for water treatment: A review," *Journal of Bioresources and Bioproducts,* vol. 6, no. 4, pp. 292-322, 2021.

[12] J. Park, M. Jung, H. Jang, K. Lee, N. F. Attia, and H. Oh, "A facile synthesis tool of nanoporous carbon for promising H_2, CO_2, and CH_4 sorption capacity and selective gas separation," *Journal of Materials Chemistry A,* vol. 6, no. 45, pp. 23087-23100, 2018.

[13] J. Park, S. Y. Cho, M. Jung, K. Lee, Y.-C. Nah, N. F. Attia, and H. Oh, "Efficient synthetic approach for nanoporous adsorbents capable of pre- and post-combustion CO_2 capture and selective gas separation," *Journal of CO_2 Utilization,* vol. 45, p. 101404, 2021.

[14] L. Luo, Y. Lan, Q. Zhang, J. Deng, L. Luo, Q. Zeng, H. Gao, and W. Zhao, "A review on biomass-derived activated carbon as electrode materials for energy storage supercapacitors," *Journal of Energy Storage,* vol. 55, p. 105839, 2022.

[15] X.-f. Tan, S.-b. Liu, Y.-g. Liu, Y.-l. Gu, G.-m. Zeng, X.-j. Hu, X. Wang, S.-h. Liu, and L.-h. Jiang, "Biochar as potential sustainable precursors for activated carbon production: Multiple applications in environmental protection and energy storage," *Bioresource Technology,* vol. 227, pp. 359-372, 2017.

[16] K. Phothong, C. Tangsathitkulchai, and P. Lawtae, "The analysis of pore development and formation of surface functional groups in bamboo-based activated carbon during CO_2 activation," *Molecules,* vol. 26, no. 18, p. 5641, 2021.

[17] A. Toprak and T. Kopac, "Carbon dioxide adsorption using high surface area activated carbons from local coals modified by KOH, NaOH and $ZnCl_2$ agents," *International Journal of Chemical Reactor Engineering,* vol. 15, no. 3, 2017.

[18] T. Lan, Y. Zhao, J. Deng, J. Zhang, L. Shi, and D. Zhang, "Selective catalytic oxidation of NH_3 over noble metal-based catalysts: State of the art and future prospects," *Catalysis Science & Technology,* vol. 10, no. 17, pp. 5792-5810, 2020.

[19] A. Linares-Solano, M. Lillo-Ródenas, J. Marco-Lozar, M. Kunowsky, and A. Romero-Anaya, "NaOH and KOH for preparing activated carbons used in energy and environmental

applications," *International Journal of Energy, Environment and Economics,* vol. 20, pp. 59-91, 2012.

[20] N. Li, J. Zhang, Z. Li, and Y. Li, "Characteristics of aerosol formation and emissions during corn stalk pyrolysis," *Energies,* vol. 13, no. 22, p. 5924, 2020.

[21] Z. Heidarinejad, M. H. Dehghani, M. Heidari, G. Javedan, I. Ali, and M. Sillanpää, "Methods for preparation and activation of activated carbon: A review," *Environmental Chemistry Letters,* vol. 18, no. 2, pp. 393-415, 2020.

[22] S. De Gisi, G. Lofrano, M. Grassi, and M. Notarnicola, "Characteristics and adsorption capacities of low-cost sorbents for wastewater treatment: A review," *Sustainable Materials and Technologies,* vol. 9, pp. 10-40, 2016.

[23] J. A. Maciá-Agulló, B. C. Moore, D. Cazorla-Amorós, and A. Linares-Solano, "Activation of coal tar pitch carbon fibres: Physical activation vs. Chemical activation," *Carbon,* vol. 42, no. 7, pp. 1367-1370, 2004.

[24] V. Smakhtin, *Impacts of rising biofuel demand on local water resources: Case studies in Thailand and Malaysia*. 2011.

[25] P. W. Tait, J. Brew, A. Che, A. Costanzo, A. Danyluk, M. Davis, A. Khalaf, K. McMahon, A. Watson, K. Rowcliff, and D. Bowles, "The health impacts of waste incineration: A systematic review," *Australian and New Zealand Journal of Public Health,* vol. 44, no. 1, pp. 40-48, 2020.

[26] E. Jaguaribe, L. Medeiros, M. Barreto, and L. Araujo, "The performance of activated carbons from sugarcane bagasse, babassu, and coconut shells in removing residual chlorine," *Brazilian Journal of Chemical Engineering - Brazilian Journal of Chemical Engineering,* vol. 22, 2005.

[27] X. Yuan, B. Liu, J. Xu, X. Yang, K. Zeinu, X. He, L. Wu, J. Hu, J. Yang, and J. Xie, "Lamellar mesoporous carbon derived from bagasse for the cathode materials of lithium-sulfur batteries," *RSC Advances,* vol. 7, no. 22, pp. 13595-13603, 2017.

[28] D. B. Babu and K. Ramesha, "Melamine assisted liquid exfoliation approach for the synthesis of nitrogen doped graphene-like carbon nano sheets from bio-waste bagasse material and its application towards high areal density Li-S batteries," *Carbon,* vol. 144, pp. 582-590, 2019.

[29] J. Ma, L. Yang, X. Yang, Y. Li, E. Zhao, S. Fan, G. Xu, T. Lou, and H. Niu, "Bagasse as a carbon structure with high sulfur content for lithium-sulfur batteries," *RSC Advances,* vol. 10, no. 54, pp. 32345-32349, 2020.

[30] D. Bosubabu, R. Sampathkumar, G. Karkera, and K. Ramesha, "Facile approach to prepare multiple heteroatom-doped carbon material from bagasse and its applications toward lithium-ion and lithium−sulfur batteries," *Energy and Fuels,* vol. 35, no. 9, pp. 8286-8294, 2021.

[31] R. Luan, D. Xu, H. Pan, C. Zhu, D. Wang, X. Meng, Y. Li, M. Imtiaz, S. Zhu, and J. Ma, "High electrochemical cycling performance through accurately inheriting hierarchical porous structure from bagasse," *Journal of Energy Storage,* vol. 22, pp. 60-67, 2019.

[32] K. Nanaji, B. V. Sarada, U. V. Varadaraju, T. N Rao, and S. Anandan, "A novel approach to synthesize porous graphene sheets by exploring koh as pore inducing agent as well as a catalyst for supercapacitors with ultra-fast rate capability," *Renewable Energy,* vol. 172, pp. 502-513, 2021.

[33] E. Yagmur, Y. Gokce, S. Tekin, N. I. Semerci, and Z. Aktas, "Characteristics and comparison of activated carbons prepared from oleaster (elaeagnus angustifolia l.) fruit using KOH and $ZnCl_2$," *Fuel,* vol. 267, p. 117232, 2020.

[34] N. A. Zubbri, A. Mohamed, P. Lahijani, and M. Mohammadi, "Low temperature CO_2 capture on biomass-derived KOH-activated hydrochar established through hydrothermal carbonization with water-soaking pre-treatment," *Journal of Environmental Chemical Engineering,* vol. 9, p. 105074, 2021.

[35] H. Mao, X. Chen, R. Huang, M. Chen, R. Yang, P. Lan, M. Zhou, F. Zhang, Y. Yang, and X. Zhou, "Fast preparation of carbon spheres from enzymatic hydrolysis lignin: Effects of hydrothermal carbonization conditions," *Scientific Reports,* vol. 8, no. 1, p. 9501, 2018.

[36] T. Mwenya, H. Fan, H. Dai, and M. Li, "The detailed evolution of carbon spheres by hydrothermal method," *International Journal of Photoenergy,* vol. 2016, p. 9057418, 2016.

[37] H. Rustamaji, T. Prakoso, H. Devianto, P. Widiatmoko, and W. H. Saputera, "Urea nitrogenated mesoporous activated carbon derived from oil palm empty fruit bunch for high-performance supercapacitor," *Journal of Energy Storage,* vol. 52, p. 104724, 2022.

[38] X.-Y. Liu, M. Huang, H.-L. Ma, Z.-Q. Zhang, J.-M. Gao, Y.-L. Zhu, X.-J. Han, and X.-Y. Guo, "Preparation of a carbon-based solid acid catalyst by sulfonating activated carbon in a chemical reduction process," *Molecules,* vol. 15, no. 10, pp. 7188-7196, 2010.

[39] R. B. González-González, L. T. González, S. Iglesias-González, E. González-González, S. O. Martinez-Chapa, M. Madou, M. M. Alvarez, and A. Mendoza, "Characterization of chemically activated pyrolytic carbon black derived from waste tires as a candidate for nanomaterial precursor," *Nanomaterials,* vol. 10, no. 11, 2020.

[40] V. Ferreira-Leitão, C. C. Perrone, J. Rodrigues, A. P. M. Franke, S. Macrelli, and G. Zacchi, "An approach to the utilisation of CO_2 as impregnating agent in steam pretreatment of sugar cane bagasse and leaves for ethanol production," *Biotechnology for Biofuels,* vol. 3, no. 1, p. 7, 2010.

[41] F. R. M. S. Raj, G. Boopathi, N. V. Jaya, D. Kalpana, and A. Pandurangan, "N, s codoped activated mesoporous carbon derived from the datura metel seed pod as active electrodes for supercapacitors," *Diamond and Related Materials,* vol. 102, p. 107687, 2020.

[42] J. Ma, L. Yang, X. Yang, Y. Li, E. Zhao, S. Fan, G. Xu, T. Lou, and H. Niu, "Bagasse as a carbon structure with high sulfur content for lithium–sulfur batteries," *RSC Advances,* vol. 10, no. 54, pp. 32345-32349, 2020.

[43] F. Qin, K. Zhang, J. Fang, Y. Lai, Q. Li, Z. Zhang, and J. L, "High performance lithium sulfur batteries with a cassava-derived carbon sheet as a polysulfides inhibitor," *New J. Chem.,* vol. 38, 2014.

[44] F. Chen, L. Ma, J. Ren, X. Luo, B. Liu, and X. Zhou, "Sandwich-type nitrogen and sulfur codoped graphene-backboned

porous carbon coated separator for high performance lithium-sulfur batteries," (in eng), *Nanomaterials (Basel),* vol. 8, no. 4, 2018.

[45] P. Treeweranuwat, P. Boonyoung, M. Chareonpanich, and K. Nueangnoraj, "Role of nitrogen on the porosity, surface, and electrochemical characteristics of activated carbon," *ACS Omega,* vol. 5, no. 4, pp. 1911-1918, 2020.

[46] Y. Hu, W. Chen, T. Lei, Y. Jiao, J. Huang, C. Gong, C. Yan, X. Wang, and J. Xiong, "Strategies toward high-loading lithium-sulfur battery," *Advanced Energy Materials,* p. 2000082, 2020.

[47] M. Yang, N. Jue, Y. Chen, and Y. Wang, "Improving cyclability of lithium metal anode via constructing atomic interlamellar ion channel for lithium sulfur battery," *Nanoscale Research Letters,* vol. 16, no. 1, 2021.

[48] M. Yang, N. Jue, Y. Chen, and Y. Wang, "Improving cyclability of lithium metal anode via constructing atomic interlamellar ion channel for lithium sulfur battery," *Nanoscale Research Letters,* vol. 16, no. 1, p. 52, 2021.

[49] Y. Hu, W. Chen, T. Lei, B. Zhou, Y. Jiao, Y. Yan, X. Du, J. Huang, C. Wu, X. Wang, Y. Wang, B. Chen, J. Xu, C. Wang, and J. Xiong, "Carbon quantum dots–modified interfacial interactions and ion conductivity for enhanced high current density performance in lithium–sulfur batteries," *Advanced Energy Materials,* vol. 9, no. 7, p. 1802955, 2019.